

Submitted to 11nd Aix en Provence Conference

Session 8 : Elastic Scattering and low Multiplicities

BNL 18183

CONF-730943--2

AMPLITUDE ANALYSIS OF HYPERCHARGE EXCHANGE REACTIONS

R.D. Field, S.U. Chung *
Brookhaven National Laboratory

R.L. Eisner
CERN

A. Rougé, H. Vidéau
Ecole Polytechnique, Paris

M. Aguilar Benitez, F. Barreiro, J. Rubio
Junta de Energia Nuclear - Madrid

J.P. de Brion, L. Moscoso
D Ph PE, Saclay

* Part of the research carried out at Brookhaven National Laboratory
under the auspices of the U.S. Atomic Energy Commission.

NOTICE

This report was prepared as an account of work sponsored by the United States Government. Neither the United States nor the United States Atomic Energy Commission, nor any of their employees, nor any of their contractors, subcontractors, or their employees, makes any warranty, express or implied, or assumes any legal liability or responsibility for the accuracy, completeness or usefulness of any information, apparatus, product or process disclosed, or represents that its use would not infringe privately owned rights.

MASTER

DISTRIBUTION OF THIS DOCUMENT IS UNLIMITED

leg

In this paper we present results on a transversity amplitude analysis of final states produced in K^-p interactions. The sample derives from combined data of Brookhaven National Laboratory (3.9 - 4.6 GeV/c)¹ and Ecole Polytechnique - Saclay (3.95 GeV/c)² and corresponds, after efficiency corrections, to a total of ~ 20 events/ μ b.

The final states of interest are :

$$K^-p \rightarrow \Lambda \Psi \quad (1)$$

$$K^-p \rightarrow \Lambda \omega \quad (2)$$

$$K^-p \rightarrow \Upsilon^{*+}(1385)\pi^- \quad (3)$$

Results on the BNL analysis of reactions (1) and (2) can be found in Ref. 3 , and that of reaction (3) in Ref. 4[†] . More details on formalism used in the present work can be found in the two references.

In Sect. I the amplitude analysis is presented on reaction (1) and (2), and the data on the $K^-p \rightarrow \Lambda \Psi$ reaction is compared with previous analysis on the reaction $\pi^-p \rightarrow \Lambda K^*(890)$. In Sect. II the corresponding analysis on reaction (3) is presented and comparison made with expectations of quark and duality predictions.

I.- VECTOR MESON PRODUCTION

$$P B \rightarrow V B'$$

The transversity frame is defined with z axis normal to the production plane (i.e., $\hat{n} = \vec{p}_p \times \vec{p}_V / |\vec{p}_p \times \vec{p}_V|$). The y axis is chosen either in the direction of the resonance $V(B')$ as seen in the c.m. frame (helicity-transversity frame) or in the direction of the incoming pseudoscalar meson (target proton) in the rest frame of the vector meson $V(B')$ (Jackson-transversity frame) ;

There are 12 complex transversity amplitudes which describe $PB \rightarrow V B'$ scattering. These we define as ,

$$T_{\lambda'\lambda}^{\mu}$$

where μ , λ' and λ measure the component of spin along the transversity z axis of the V, B' and B, respectively. Parity conservation in the production process gives,

$$T_{\lambda'\lambda}^{\mu} = (-1)^{\lambda' - \lambda + \mu} T_{\lambda\lambda'}^{\mu}$$

so that six complex amplitudes (12 numbers) are sufficient to describe the reaction. It is convenient to form linear combinations of the $T_{\lambda\lambda'}^{\mu}$ and form so called Byers and Yang amplitudes :

$$\begin{aligned} T_{++}^0 &= -i(2)^{1/2} A^+ & T_{--}^0 &= -i(2)^{1/2} A^- \\ T_{-+}^1 &= iB^+ + C^+ & T_{+-}^1 &= iB^- + C^- \\ T_{-+}^{-1} &= -iB^+ + C^+ & T_{+-}^{-1} &= -iB^- + C^- \end{aligned}$$

Now, what we actually measure are the density matrix elements which in the transversity frame are related to bilinear products of the transversity amplitudes,

$$T_{nn'}^{mm'}(V, B') = \sum_{\lambda} T_{n\lambda}^m T_{n'\lambda}^{m' *} / \Sigma$$

$$\Sigma = \sum_{\mu, \lambda', \lambda} |T_{\lambda\lambda'}^{\mu}|^2$$

so that, since we sum over the initial baryon spin states we obtain no information about the phase between states with proton transversity up and down (i.e. $\lambda = -1/2$ and $\lambda = +1/2$), and the transversity amplitudes and the corresponding Byers and Yang type amplitudes naturally separate into two groups :

$$\begin{pmatrix} T_{++}^0 \\ T_{-+}^1 \\ T_{-+}^{-1} \end{pmatrix} \quad \text{and} \quad \begin{pmatrix} T_{--}^0 \\ T_{+-}^1 \\ T_{+-}^{-1} \end{pmatrix} \quad \text{or} \quad \begin{pmatrix} A^+ \\ B^+ \\ C^+ \end{pmatrix} \quad \text{and} \quad \begin{pmatrix} A^- \\ B^- \\ C^- \end{pmatrix}$$

The relative phases between numbers in each group is then readily obtained, but no information is available on the overall phase am^1 , as mentioned above, between the $\lambda = +1/2$ and $\lambda = -1/2$ group. Therefore, 10 out of the 12 numbers needed to totally specify the reaction can be obtained.

The Jackson (or helicity) density matrix elements are written in terms of the Jackson (or helicity) Byers-Yang A, B, C as follows :

$$\begin{aligned} \rho_{11} - \rho_{00} &= (|A^+|^2 + |A^-|^2 + |B^+|^2 + |B^-|^2 \\ &\quad - 2|C^+|^2 - 2|C^-|^2)/\Sigma, \\ \text{Re}\rho_{10} &= +\sqrt{2} \text{Re}(B^+C^{*-} + B^-C^{*+})/\Sigma, \\ \rho_{1,-1} &= (|A^+|^2 + |A^-|^2 - |B^+|^2 - |B^-|^2)/\Sigma, \\ \rho &= 2(|A^+|^2 - |A^-|^2 - |B^+|^2 + |B^-|^2 \\ &\quad - |C^+|^2 + |C^-|^2)/\Sigma, \\ C_1 &= (|A^+|^2 - |A^-|^2 - |B^+|^2 + |B^-|^2 \\ &\quad + 2|C^+|^2 - 2|C^-|^2)/\Sigma, \\ C_2 &= \sqrt{2} \text{Im}(A^+C^{*-} + A^-C^{*+})/\Sigma, \\ C_3 &= \text{Im}(A^+B^{*-} + A^-B^{*+})/\Sigma, \\ C_4 &= +2 \text{Re}(A^+B^{*-} + A^-B^{*+})/\Sigma, \\ C_5 &= (-|A^+|^2 + |A^-|^2 - |B^+|^2 + |B^-|^2)/\Sigma, \\ C_6 &= -\sqrt{2} \text{Re}(A^+C^{*-} + A^-C^{*+})/\Sigma, \\ C_7 &= -\sqrt{2} \text{Re}(B^+C^{*-} + B^-C^{*+})/\Sigma. \end{aligned}$$

Where

$$\begin{aligned} \Sigma &= 2(|A^+|^2 + |A^-|^2 + |B^+|^2 \\ &\quad + |B^-|^2 + |C^+|^2 + |C^-|^2). \end{aligned}$$

and

$$\begin{aligned} C_1 &= \text{Im}\rho_{10}^{00} - \text{Im}\rho_{10}^{11}, \\ C_2 &= \text{Im}\rho_{10}^{10} - \text{Im}\rho_{10}^{01}, \\ C_3 &= \text{Im}\rho_{10}^{1,-1}, \\ C_4 &= \text{Im}\rho_{10}^{1,-1} + \text{Im}\rho_{10}^{0,-1}, \\ C_5 &= \text{Im}\rho_{10}^{1,-1} - \text{Im}\rho_{10}^{0,-1}, \\ C_6 &= \text{Im}\rho_{10}^{10} + \text{Im}\rho_{10}^{01}, \\ C_7 &= \text{Im}\rho_{10}^{10} - \text{Im}\rho_{10}^{01}. \end{aligned}$$

The angular distribution of the decay vector meson V and baryon B' , applicable in the s -channel helicity and Jackson frames, can be written in terms of the joint density-matrix elements and angles θ, φ (θ', φ') which describe the decay of the vector meson (baryon B') as

$$W(\theta, \varphi, \theta', \varphi') = \left(\frac{1}{16\pi^2} \right) (W_0 + W_1 + W_2 + W_3 + W_4 + W_5 + W_6 + W_7 + W_8 + W_9 + W_{10} + W_{11}),$$

where

$$\begin{aligned} W_0 &= (1 - 3 \cos^2 \theta) \rho_{11} - \rho_{00}, \\ W_1 &= -3/2 \sin^2 \theta \cos \theta \operatorname{Re} \rho_{10}, \\ W_2 &= -3 \sin^2 \theta \cos^2 \theta \rho_{1-1}, \\ W_3 &= \alpha \sin \theta' \sin \varphi' C_1, \\ W_4 &= 2\alpha (1 - 3 \cos^2 \theta) \sin \theta' \sin \varphi' C_1, \\ W_5 &= 3\sqrt{2} \alpha \cos \theta' \sin 2\theta \sin \varphi' C_2, \\ W_6 &= 6\alpha \cos \theta' \sin^2 \theta \sin 2\varphi' C_3, \\ W_7 &= 3\alpha \sin \theta' \sin^2 \theta \sin 2\varphi' \cos \varphi' C_4, \\ W_8 &= 3\alpha \sin \theta' \sin^2 \theta \cos 2\varphi' \sin \varphi' C_5, \\ W_{10} &= 3\alpha \sin \theta' \sqrt{2} \sin 2\theta \sin \varphi' \cos \varphi' C_6, \\ W_{11} &= 3\alpha \sin \theta' \sqrt{2} \sin 2\theta \cos \varphi' \sin \varphi' C_7. \end{aligned}$$

Note that by using this amplitude analysis the positivity conditions among the $\rho_{\lambda\lambda'}$ are automatically satisfied.

In addition, tests on the quality of the data can be made since the $\left| T_{\lambda\lambda}^p \right|^2$ are invariant under rotation around the z -axis and therefore, should be the same in both the Jackson and helicity transversity frames.

One of the reasons for introducing the Λ , B and C parameters is that they are simply related to the nice physics quantities one wants to extract, e.g.:

Natural Parity Exchange Contributions

$$C_1 \Sigma = \left| \Lambda^- \right|^2 + \left| \Lambda^+ \right|^2 \quad ; \quad T_1 \Sigma = \left| \Lambda^+ \right|^2 - \left| \Lambda^- \right|^2$$

Unnatural Parity Exchange Contributions

$$\rho^{\pm} = |B^+|^2 + |B^-|^2; \quad \Gamma_2^{\pm} = |B^-|^2 - |B^+|^2$$

$$\rho_{00}^{\pm} = |C^+|^2 + |C^-|^2; \quad \Gamma_3^{\pm} = |C^-|^2 - |C^+|^2$$

with the polarization, $\rho^{\pm} = \Gamma_1 + \Gamma_2 + \Gamma_3$.

Maximum likelihood fits to the data were performed with the above expression for the angular distribution.

The values of the Byers-Yang amplitudes as a function of momentum transfer for the reactions $K^-p \rightarrow \Lambda \phi$ are shown in Fig. 3.4 BC in the Jackson transversity and Fig. 3.4 DE in the helicity transversity frame. The corresponding distributions for the reaction $K^-p \rightarrow \Lambda \omega$ are shown in Fig 1.2 BC and Fig 1.2 DE respectively. As previously observed, there is a large difference between the amplitude structure of the two reactions. In particular in contrast to $K^-p \rightarrow \Lambda \omega$ for $K^-p \rightarrow \Lambda \phi$ one observes large values of $|A^-|^2$ and small values of $|A^+|^2$ as a function of momentum transfer. This essentially produces the observed difference in the sign of the polarization of the two reactions; that in $K^-p \rightarrow \Lambda \omega$ is found to be large and positive in contrast to the negative polarization found in $K^-p \rightarrow \Lambda \phi$. In the case of the $K^-p \rightarrow \Lambda \omega$ reaction it is found (see Fig 3), that within error, in both the helicity and Jackson transversity system that C^- and B^- are in phase. This along with the observed small value of $|B^+|^2$ in both frames results in the saturation of the spin one positivity condition (fig. 6) :

$$2 (\text{Re } \rho_{10})^2 \leq \rho_{00} (\rho_{11} - \rho_{1-1})$$

in both the Jackson and helicity frames. Such a result is not found in the $K^-p \rightarrow \Lambda \phi$ case.

In Fig. 5 are shown the values of the square of the Byers Yang amplitude from the reaction $K^-p \rightarrow \Lambda \phi$ along with the corresponding analysis for $K^-p \rightarrow \Lambda \omega$ (see) at 3.9 and 4.5 GeV/c. In agreement with simple SU(3) and quark model prediction the amplitude structure is observed to be identical for the two reactions.

II.- $K^- p \rightarrow Y^{*+} (1385) \pi^-$

The reaction $K^- p \rightarrow Y^{*+} (1385) \pi^-$ can be described by four complex transversity amplitudes, $T_{2\mu, 2\mu'}$ where μ (μ') corresponds to the spin of the Y^* (proton) along the transversity $-z$ axis. From the decay correlations the magnitudes of the four amplitudes $|T_{3-1}|$, $|T_{11}|$, $|T_{-1-1}|$, and $|T_{-31}|$ as well as the two phases :

$$\begin{aligned} \delta_1 &= \text{phase between } T_{3-1} \text{ and } T_{-1-1} \\ \delta_2 &= \text{phase between } T_{11} \text{ and } T_{-31} \end{aligned}$$

can be obtained. Their extraction leads to a determination of the full density matrix (I;E real and imaginary parts of all $\rho_{mm'}$) in both the transversity and helicity frames through the relation

$$\rho_{2m', 2m} = \sum_{\lambda} T_{2m-, 2\lambda} T_{2m', 2\lambda}^*$$

In the present analysis :

1/ A massdependent maximum likelihood fit of the joint decay angular distribution is performed. The resonance part is parametrized in terms of the transversity density matrix element $\rho_{2m, 2m'}$ as shown above. The joint decay angular distribution (valid in any transversity frame) is written as follows :

$$W(\theta, \varphi, \theta', \varphi') = \frac{1}{16\pi} v^{-2} (W_1 \rho_{33} + W_2 \rho_{11} + W_3 \rho_{-1-1} + i W_4 \rho_{-3-3} + W_5 \text{Re} \rho_{3-1} + W_6 \text{Im} \rho_{3-1} + W_7 \text{Re} \rho_{1-3} + W_8 \text{Im} \rho_{1-3})$$

$$\begin{aligned}
W_1 &= \frac{1}{2}(\sin^2\theta + \alpha \sin^2\theta \cos\theta \cos\theta' - \alpha \sin^2\theta \sin\theta' \cos\varphi'), \\
W_2 &= \frac{1}{2}[(1 + 3\cos^2\theta) + \alpha \cos\theta \cos\theta'(9\cos^2\theta - 5) + \alpha \sin\theta \sin\theta' \cos\varphi'(1 - 9\cos^2\theta)], \\
W_3 &= \frac{1}{2}[(1 + 3\cos^2\theta) - \alpha \cos\theta \cos\theta'(9\cos^2\theta - 5) - \alpha \sin\theta \sin\theta' \cos\varphi'(1 - 9\cos^2\theta)], \\
W_4 &= \frac{1}{2}(\sin^2\theta - \alpha \sin^2\theta \cos\theta \cos\theta' + \alpha \sin^2\theta \sin\theta' \cos\varphi'), \\
W_5 &= -\sqrt{3}[\sin^2\theta \cos 2\varphi + 3\alpha \sin^2\theta \cos\theta \cos 2\varphi \cos\theta' \\
&\quad - \alpha \sin\theta \sin\theta'(\cos 2\varphi \cos\varphi' - 3\cos^2\theta \cos\varphi' \cos 2\varphi + 2\cos\theta \sin\varphi' \sin 2\varphi)], \\
W_6 &= \sqrt{3}[\sin^2\theta \sin 2\varphi + 3\alpha \sin^2\theta \cos\theta \sin 2\varphi \cos\theta' \\
&\quad - \alpha \sin\theta \sin\theta'(\sin 2\varphi \cos\varphi' - 3\cos^2\theta \cos\varphi' \sin 2\varphi - 2\cos\theta \sin\varphi' \cos 2\varphi)], \\
W_7 &= \sqrt{3}[\sin^2\theta \cos 2\varphi - 3\alpha \sin^2\theta \cos\theta \cos 2\varphi \cos\theta' \\
&\quad + \alpha \sin\theta \sin\theta'(\cos 2\varphi \cos\varphi' - 2\cos^2\theta \cos\varphi' \cos 2\varphi + 2\cos\theta \sin\varphi' \sin 2\varphi)], \\
W_8 &= \sqrt{3}[\sin^2\theta \sin 2\varphi - 3\alpha \sin^2\theta \cos\theta \sin 2\varphi \cos\theta' \\
&\quad + \alpha \sin\theta \sin\theta'(\sin 2\varphi \cos\varphi' - 3\cos^2\theta \cos\varphi' \sin 2\varphi - 2\cos\theta \sin\varphi' \cos 2\varphi)],
\end{aligned}$$

where α is the Λ decay asymmetry parameter ($=0.645$), and where θ and φ refer to the polar and azimuthal angles, respectively, of the decay Λ in the Y^* (1385) rest system with the z axis normal to the production plane; θ' and φ' are the corresponding angles for the decay proton in the Λ rest frame with the z' axis along the Λ direction in the Y^* (1385) rest frame.

To impose the trace condition automatically we write the squared amplitudes in term of auxiliary parameters, x_i , as follow :

$$\begin{aligned}
|T_{3-1}|^2 &= x_1 \\
|T_{11}|^2 &= (1-x_1)x_2 \\
|T_{-1-1}|^2 &= (1-x_1)(1-x_2)x_3 \\
|T_{-31}|^2 &= (1-x_1)(1-x_2)(1-x_3) \\
\sigma_1 &= x_4 \\
\delta_2 &= x_5
\end{aligned}$$

with $0 \leq x_i \leq 1$ $i=1,3$

and that

$$|T_{3-1}|^2 + |T_{11}|^2 + |T_{-1-1}|^2 + |T_{-31}|^2 = 1$$

The fit was performed in the helicity transversity with the x_i as parameters. The squared amplitudes and phases were then calculated and the errors properly obtained. The values of the amplitudes and their respective phases are shown in Fig. 7 along with the values of the transversity density matrix elements obtained through () above :

$$\begin{aligned} \rho_{33}^T &= |T_{3-1}|^2 \\ \rho_{11}^T &= |T_{11}|^2 \\ \rho_{-1-1}^T &= |T_{-1-1}|^2 \\ \rho_{-3-3}^T &= |T_{-31}|^2 \end{aligned}$$

$$\begin{aligned} \text{Re } \rho_{3-1}^T &= |T_{3-1}| |T_{-1-1}| \cos \delta_1 \\ \text{Im } \rho_{3-1}^T &= |T_{3-1}| |T_{-1-1}| \sin \delta_1 \\ \text{Re } \rho_{1-3}^T &= |T_{11}| |T_{-31}| \cos \delta_2 \\ \text{Im } \rho_{1-3}^T &= |T_{11}| |T_{-31}| \sin \delta_2 \end{aligned}$$

The density matrix elements, so obtained, are shown in Fig. 8. The simple non relativistic quark model predicts :

$$\begin{aligned} T_{11} &= T_{-1-1} \\ T_{3-1} &= T_{-31} = 0.0 \end{aligned}$$

so giving

$$\rho_{11}^T = \rho_{-1-1}^T = \frac{1}{2}$$

with all other $\rho_{mm'}^T = 0.0$. These predictions give the dotted curves shown in fig. 8. Whereas the gross features of the data are in accord with the prediction. There are, as previously reported, some violations. In particular, ρ_{33}^T and both $\text{Re } \rho_{3-1}^T$ and $\text{Im } \rho_{3-1}^T$ are observed to be non-zero in

the region - $t^1 < 0.3 \text{ GeV}^2$.

We have rotated the transversity density matrix elements obtained above (which satisfy all positivity requirements) in order to obtain the helicity density matrix elements. The error on the latter values are obtained in a similar fashion.

The relation between the density matrix element is given by :

$$\begin{aligned} \text{Re } \rho_{33}^H &= [\text{Re } \rho_{33}^T + \text{Re } \rho_{3-3}^T + 2(\text{Re } \rho_{11}^T + \text{Re } \rho_{1-1}^T) - 2\sqrt{3}(\text{Re } \rho_{3-1}^T + \text{Re } \rho_{1-3}^T)]/8 \\ \text{Re } \rho_{31}^H &= [\text{Im } \rho_{3-1}^T + \text{Im } \rho_{1-3}^T]/2 \\ \text{Im } \rho_{31}^H &= [\sqrt{3}(-\text{Re } \rho_{33}^T - \text{Re } \rho_{3-3}^T - \text{Re } \rho_{11}^T + \text{Re } \rho_{1-1}^T) + 2(\text{Re } \rho_{3-1}^T - \text{Re } \rho_{1-3}^T)]/8 \\ \text{Re } \rho_{3-1}^H &= [\sqrt{3}(-\text{Re } \rho_{33}^T - \text{Re } \rho_{3-3}^T + \text{Re } \rho_{11}^T + \text{Re } \rho_{1-1}^T) + 2(\text{Re } \rho_{3-1}^T + \text{Re } \rho_{1-3}^T)]/8 \\ \text{Im } \rho_{3-1}^H &= [-\text{Im } \rho_{3-1}^T + \text{Im } \rho_{1-3}^T]/2 \\ \text{Im } \rho_{3-3}^H &= [\text{Re } \rho_{33}^T - \text{Re } \rho_{3-3}^T - 2(\text{Re } \rho_{11}^T + \text{Re } \rho_{1-1}^T) - 2\sqrt{3}(\text{Re } \rho_{3-1}^T - \text{Re } \rho_{1-3}^T)]/8 \\ \text{Im } \rho_{1-1}^H &= [-2(\text{Re } \rho_{33}^T - \text{Re } \rho_{3-3}^T) + \text{Re } \rho_{11}^T - \text{Re } \rho_{1-1}^T - 2\sqrt{3}(\text{Re } \rho_{3-1}^T - \text{Re } \rho_{1-3}^T)]/8 \end{aligned}$$

The helicity frame ρ_{mm}^H , are shown in Fig. 8. Again the full density matrix is extracted. The simple quark model predictions are indicated as they dotted curves in the figure. Here, the values of $\text{Re } \rho_{31}^H$ and $\text{Re } \rho_{3-1}^H$ are in disagreement with the prediction for - $t < 0.3 \text{ GeV}^2$. In addition, there appears to be some violation ($\sim 3\sigma$) between the experimentally determined and predicted value of $\text{Im } \rho_{31}^H$. It should be noted that duality arguments predict the s-channel helicity frame amplitudes for $K^+p \rightarrow Y^* \pi^-$ to be purely real and, therefore, that $\text{Im } \rho_{mm}^H = 0.0$.

°°°°°°°

We thank Dr N.P. Samios for kindly allowing us to use the ENL data.

°°°°°°°

TABLES

Table I. Values of the Byers-Yang type amplitudes for $K^-p \rightarrow \omega\Lambda$
 $\theta_A = \text{Arg } (A)$, $\theta_B = \text{Arg } (-B)$, $\theta_C = \text{Arg } (C)$.

Table II. Values of the Byers-Yang type amplitudes for $K^-p \rightarrow \phi\Lambda$
 $\theta_A = \text{Arg } (A)$, $\theta_B = \text{Arg } (-B)$, $\theta_C = \text{Arg } (C)$

Table III. Transversity amplitudes and transversity density matrix elements for the reaction $K^-p \rightarrow \pi^- Y^{*+}(1385)$

Table IV. The s-channel helicity density matrix elements for the reaction $K^-p \rightarrow \pi^- Y^{*+}(1385)$.

REFERENCES

- 1/ M. Aguilar-Benitez et al. Phys. Rev. D6 (1972) 29
 - 2/ A. Rougé et al. N.P. B44 (1972) 365-389
 - 3/ R.D. Field et al. Phys. Rev. D7 (1973) 2036
 - 4/ M. Aguilar-Benitez et al. Phys. Rev. Let. 29 (1972) 749.
- A review of this analysis has been presented by R.D. Field at the Int. Conf. on $\pi\pi$ Scattering, Florida, State Univ. 1973 and by R.L. Eisner at the International Winter Meeting on Fundamental Physics, Formigal Spain (1973).

TABLE I

	0./1	.1/.2	.2/.4	.4/.6	.6/10	
$ A^- ^2$.03 ± .03	.23 ± .10	.07 ± .08	.10 ± .11	.08 ± .09	
$ A^+ ^2$.23 ± .10	.30 ± .10	.42 ± .12	.64 ± .15	.70 ± .15	
$ B^- ^2$.13 ± .08	.09 ± .07	.23 ± .07	.10 ± .06	.11 ± .05	Jackson
$ B^+ ^2$.07 ± .07	.09 ± .07	.01 ± .03	.00 ± .02	.01 ± .02	
$ C^- ^2$.37 ± .12	.11 ± .07	.15 ± .08	.16 ± .06	.09 ± .04	
$ C^+ ^2$.17 ± .12	.18 ± .07	.12 ± .09	.00 ± .01	.01 ± .02	
$\theta_c^- - \theta_a^-$	1.6 ± 1.3	.1 ± 1.	.4 ± .8	1. ± 1.4	1.6 ± 1.1	
$\theta_c^+ - \theta_a^+$	-2. ± 1.	-1.5 ± .8	-2. ± .6	-	-	
$\theta_c^- - \theta_b^-$.0 ± .5	.1 ± .7	.2 ± .4	.0 ± .6	-.1 ± .6	
$\theta_c^+ - \theta_b^+$	-.9 ± .6	-1.5 ± .4	-1.1 ± 1.7	-	-	
$ B^- ^2$.02 ± .03	.03 ± .04	.10 ± .05	.19 ± .07	.16 ± .05	helicity
$ B^+ ^2$.02 ± .05	.17 ± .06	.13 ± .07	.00 ± .02	.00 ± .03	
$ C^- ^2$.48 ± .16	.18 ± .06	.26 ± .08	.07 ± .05	.04 ± .03	
$ C^+ ^2$.23 ± .17	.09 ± .03	.02 ± .05	.00 ± .02	.02 ± .03	
$\theta_c^- - \theta_a^-$	3. ± 2.	1.5 ± 1.	1.5 ± .6	2.8 ± 1.2	-2.7 ± 1.3	
$\theta_c^+ - \theta_a^+$	-2.6 ± .7	-2. ± .9	- 2.4 ± .8	-	-	
$\theta_c^- - \theta_b^-$	-3.1 ± 1.5	-3.1 ± .7	2.9 ± .7	-3. ± 1.	-3.1 ± .7	
$\theta_c^+ - \theta_b^+$	-2.2 ± .9	-1.9 ± .4	-1.9 ± .8	-	-	

$$\theta_b^\pm = \text{Arg} (-B^\pm)$$

$$\theta_a^\pm = \text{Arg} (A^\pm)$$

$$\theta_c^\pm = \text{Arg} (C^\pm)$$

TABLE I

	0./1	.1/.2	.2/.4	.4/.6	.6/.1	
$ \Lambda^- ^2$.32 ± .09	.30 ± .10	.50 ± .15	.43 ± .12	.53 ± .15	
$ \Lambda^+ ^2$.03 ± .07	.12 ± .10	.01 ± .07	.05 ± .03	.01 ± .04	
$ B^- ^2$	0.5 ± .08	.07 ± .06	.07 ± .06	.03 ± .04	.07 ± .07	Jackson
$ B^+ ^2$.14 ± .10	.09 ± .07	.07 ± .06	.03 ± .04	.06 ± .06	
$ C^- ^2$.45 ± .09	.42 ± .08	.35 ± .06	.19 ± .10	.08 ± .07	
$ C^+ ^2$.01 ± .04	.00 ± .03	.00 ± .02	.27 ± .12	.25 ± .09	
$\theta_{C^-} - \theta_{a^-}$	1.9 ± .5	1.4 ± .5	.9 ± .5	1.5 ± .7	.4 ± .7	
$\theta_{C^+} - \theta_{a^+}$	-	-	-	-	-	
$\theta_{C^-} - \theta_{b^-}$	-1.9 ± .7	.1 ± .6	-1.6 ± .6	-2. ± .8	-2.1 ± .8	
$\theta_{C^+} - \theta_{b^+}$	-	-	-	-	-	
$ B^- ^2$.19 ± .08	.12 ± .06	.31 ± .06	.19 ± .12	.09 ± .07	helicity
$ B^+ ^2$.07 ± .07	.02 ± .04	.00 ± .02	.29 ± .13	.23 ± .07	
$ C^- ^2$.32 ± .09	.35 ± .10	.09 ± .08	.03 ± .05	.07 ± .05	
$ C^+ ^2$.06 ± .08	.09 ± .09	.08 ± .05	.01 ± .02	.07 ± .07	
$\theta_{C^-} - \theta_{a^-}$	2.8 ± .6	2.5 ± .6	-3. ± .4	-1.5 ± .9	-1.8 ± .6	
$\theta_{C^+} - \theta_{a^+}$	1.2 ± 2.	3. ± 1.5	-	1.5 ± 1.5	2. ± 1.6	
$\theta_{C^-} - \theta_{b^-}$	-2.7 ± .5	3.1 ± .5	-2. ± .4	-1.4 ± .7	- .9 ± .7	
$\theta_{C^+} - \theta_{b^+}$.2 ± 1.6	.2 ± 1.6		.2 ± 1.5	1.4 ± .6	

$$\theta_{b^\pm} = \text{Arg} (-B^\pm)$$

$$\theta_{a^\pm} = \text{Arg} (\Lambda^\pm)$$

$$\theta_{c^\pm} = \text{Arg} (C^\pm)$$

TABLE 3

t'	0./1	.1/.2	.2/.3	.3/.4	.4/.6	.6/.1
$ \epsilon_{3-1} ^2 = \rho_{33}$.05 ± .06	.12 ± .05	.07 ± .05	.01 ± .02	.03 ± .02	.01 ± .03
$ \epsilon_{11} ^2 = \rho_{11}$.57 ± .11	.62 ± .11	.55 ± .06	.26 ± .22	.61 ± .12	.46 ± .27
$ \epsilon_{-1-1} ^2 = \rho_{-1-1}$.38 ± .12	.20 ± .11	.37 ± .07	.71 ± .18	.33 ± .11	.54 ± .36
$ \epsilon_{-31} ^2 = \rho_{-3-3}$.00 ± .01	.06 ± .04	.01 ± .01	.03 ± .07	.02 ± .02	.00 ± .01
σ_1	2.30 ± .70	2.00 ± .39	1.88 ± .27	5.17 ± 3.38	1.61 ± .52	5.16 ± 2.48
σ_2	-.26 ± 3.20	.49 ± .31	3.76 ± 1.28	1.35 ± 1.47	3.93 ± .64	-1.50 ± 3.35
Re ρ_{3-1}	-.09 ± .09	-.06 ± .05	-.05 ± .05	.03 ± .17	.00 ± .06	.02 ± .10
In ρ_{3-1}	.10 ± .08	.14 ± .05	.15 ± .05	-.05 ± .14	.10 ± .04	-.05 ± .16
Re ρ_{1-3}	.02 ± .10	.17 ± .07	-.05 ± .05	.02 ± .13	-.08 ± .07	.00 ± .08
In ρ_{1-3}	-.01 ± .08	.09 ± .04	-.03 ± .06	.08 ± .08	-.08 ± .06	-.02 ± .09

TABLE IV

ξ	0./0.1	.1/.2	.2/.3	.3/.4	.4/.6	.6/1.
ρ_{33}	.39 ± .06	.28 ± .04	.40 ± .03	.35 ± .11	.40 ± .04	.36 ± .05
ρ_{11}	.11 ± .06	.22 ± .04	.10 ± .03	.15 ± .11	.10 ± .04	.14 ± .05
Re ρ_{31}	.05 ± .04	.12 ± .03	.06 ± .04	.02 ± .08	.01 ± .03	-.04 ± .08
Im ρ_{31}	-.08 ± .06	-.16 ± .05	-.06 ± .04	.10 ± .12	-.04 ± .04	.02 ± .15
Re ρ_{3-1}	.18 ± .05	.16 ± .03	.16 ± .03	.21 ± .05	.17 ± .02	.22 ± .03
Im ρ_{3-1}	-.06 ± .07	-.03 ± .04	-.09 ± .04	.07 ± .08	-.09 ± .04	.01 ± .11
Im ρ_{3-3}	-.02 ± .10	-.05 ± .10	-.06 ± .06	.16 ± .14	-.14 ± .12	.02 ± .19
Im ρ_{1-1}	.06 ± .06	.13 ± .06	.00 ± .02	-.05 ± .11	.00 ± .03	-.02 ± .11

FIGURES

Fig. 1. Values of the Byers-Yang type amplitudes for $K^-p \rightarrow \omega \Lambda$

A/	$ \Lambda^- ^2$	(solid)			
	$ \Lambda^+ ^2$	(dashed)			
B/	$ B^- ^2$	(solid)	$ B^+ ^2$	(dashed)	in the Jackson frame
C/	$ C^- ^2$	(solid)	$ C^+ ^2$	(dashed)	" " "
D/	$ B^- ^2$	(solid)	$ B^+ ^2$	(dashed)	in the helicity frame
E/	$ C^- ^2$	(solid)	$ C^+ ^2$	(dashed)	" " "

Fig. 2.

A/	Arg (C ⁻) - Arg (A ⁻)	(solid)	in the Jackson frame
	Arg (C ⁺) - Arg (A ⁺)	(dashed)	" " "
B/	Arg (C ⁻) - Arg (-B ⁻)	(solid)	in the Jackson frame
	Arg (C ⁺) - Arg (-B ⁺)	(dashed)	" " "
C/	Arg (C ⁻) - Arg (A ⁻)	(solid)	in the helicity frame
	Arg (C ⁺) - Arg (A ⁺)	(dashed)	" " "
d/	Arg (C ⁻) - Arg (-B ⁻)	(solid)	in the helicity frame
	Arg (C ⁺) - Arg (-B ⁺)	(dashed)	" " "

Fig. 3.

Fig. 4.

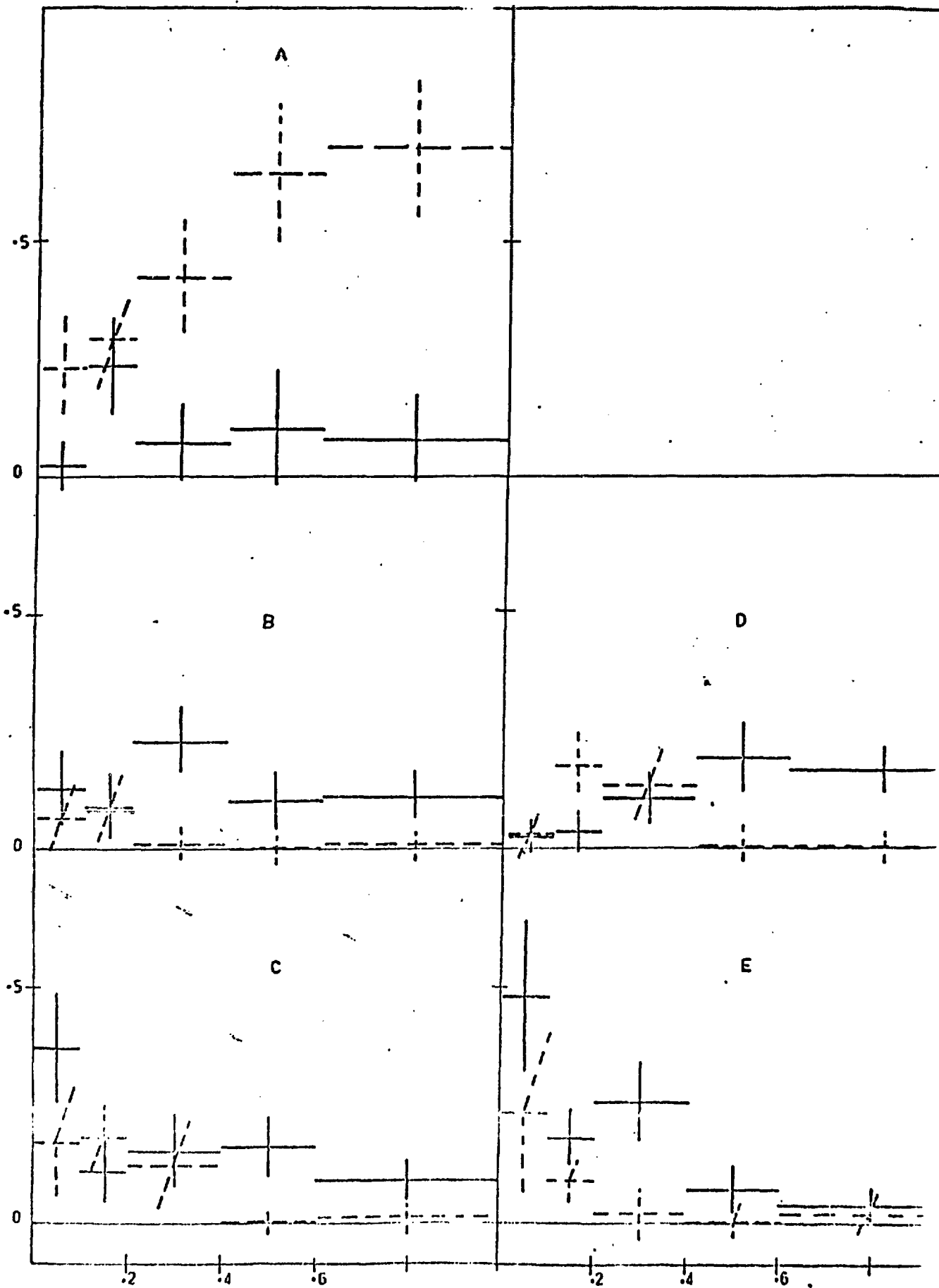
Values of the Byers-Yang type amplitudes for $K^-p \rightarrow \Psi \Lambda$

Fig. 5. Comparison of the amplitudes for $K^-p \rightarrow \Psi \Lambda$ and $\mathbb{N}^-p \rightarrow K^* \Lambda$

Fig. 6. Positivity domain for ω density matrix

Fig. 7. Transversity amplitudes and transversity density matrix elements for the reaction $K^-p \rightarrow \mathbb{N}^- Y^{*+}(1385)$

Fig. 8. The s-channel helicity density matrix elements for the reaction $K^-p \rightarrow \mathbb{N}^- Y^{*+}(1385)$.



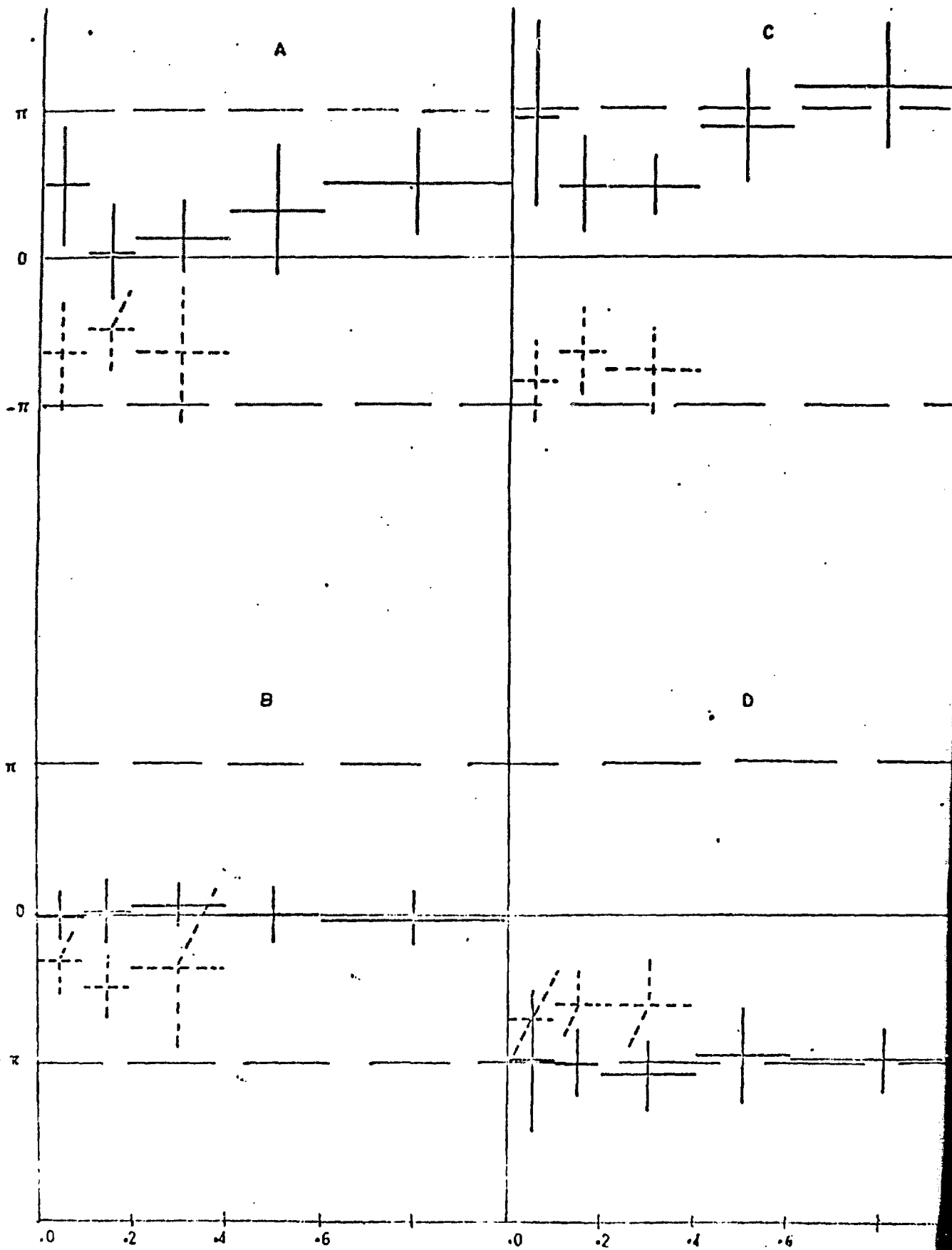


Fig. 2

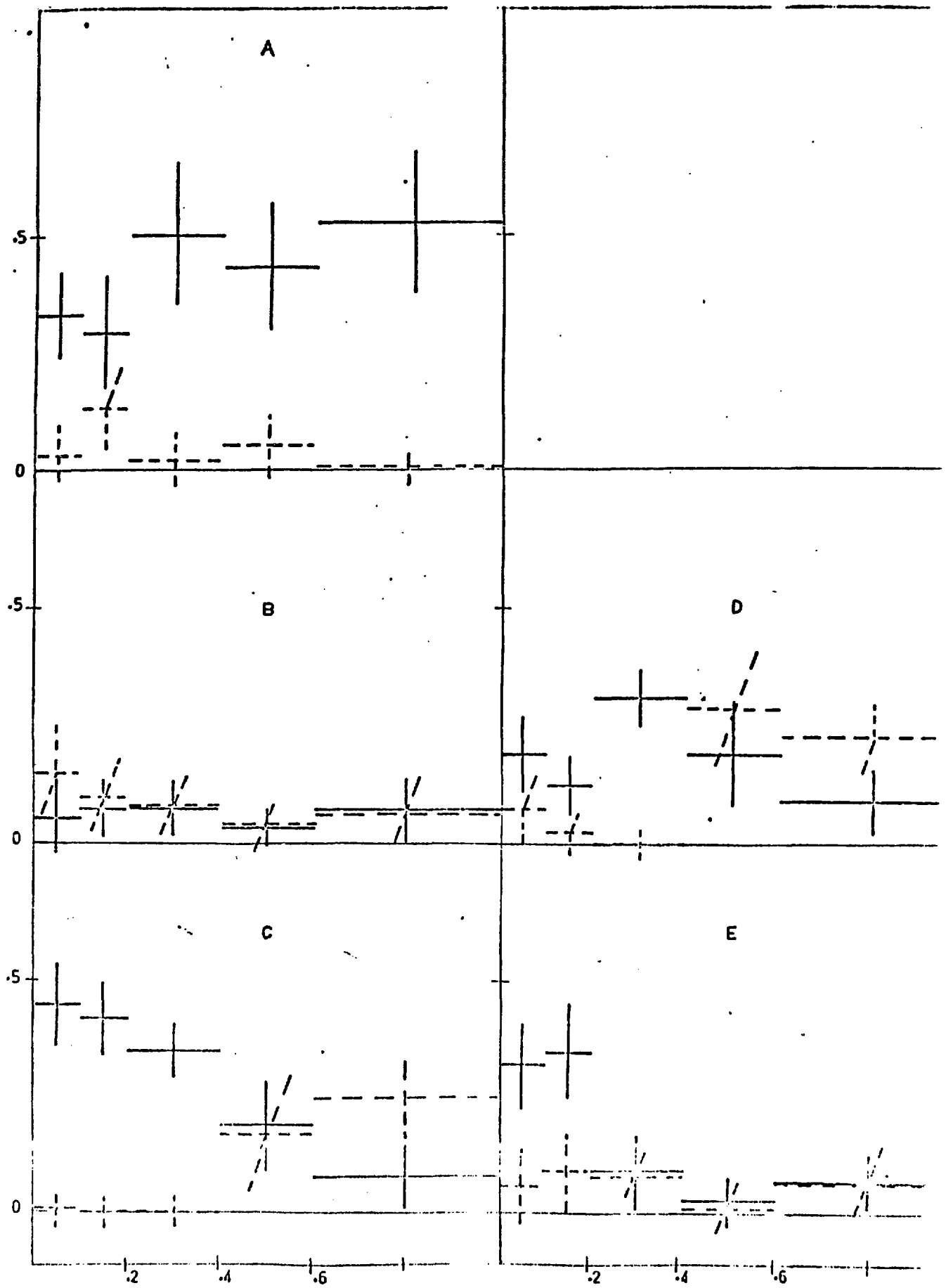
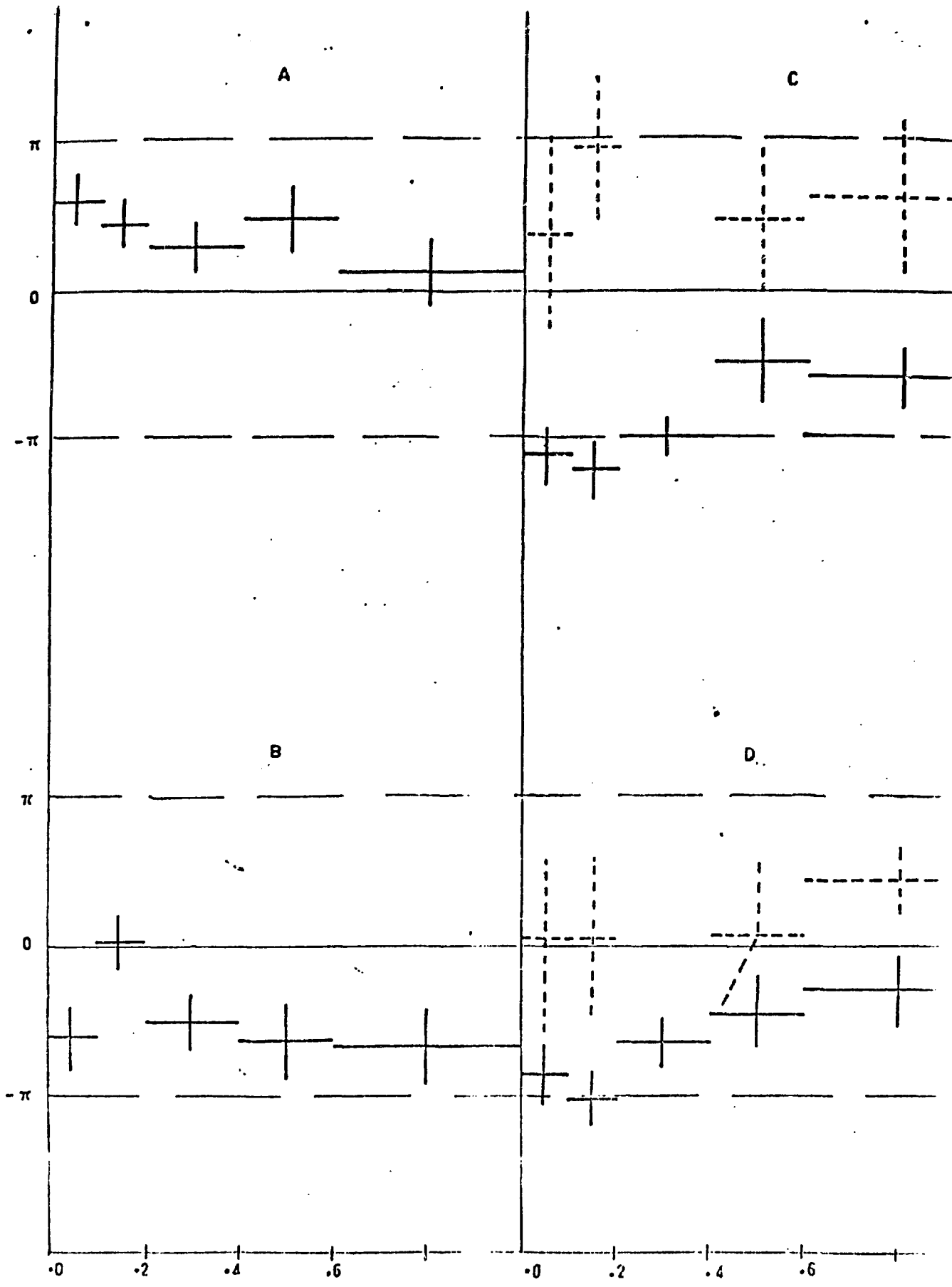


Fig. 3



$\phi \quad \pi^- p \rightarrow \kappa^{*0} \Lambda$ (BNL)
 $\psi \quad K^- p \rightarrow \phi \Lambda$ (BNL + EP) $\psi \quad \pi^- p \rightarrow K^{*0} \Lambda$ (CERN)

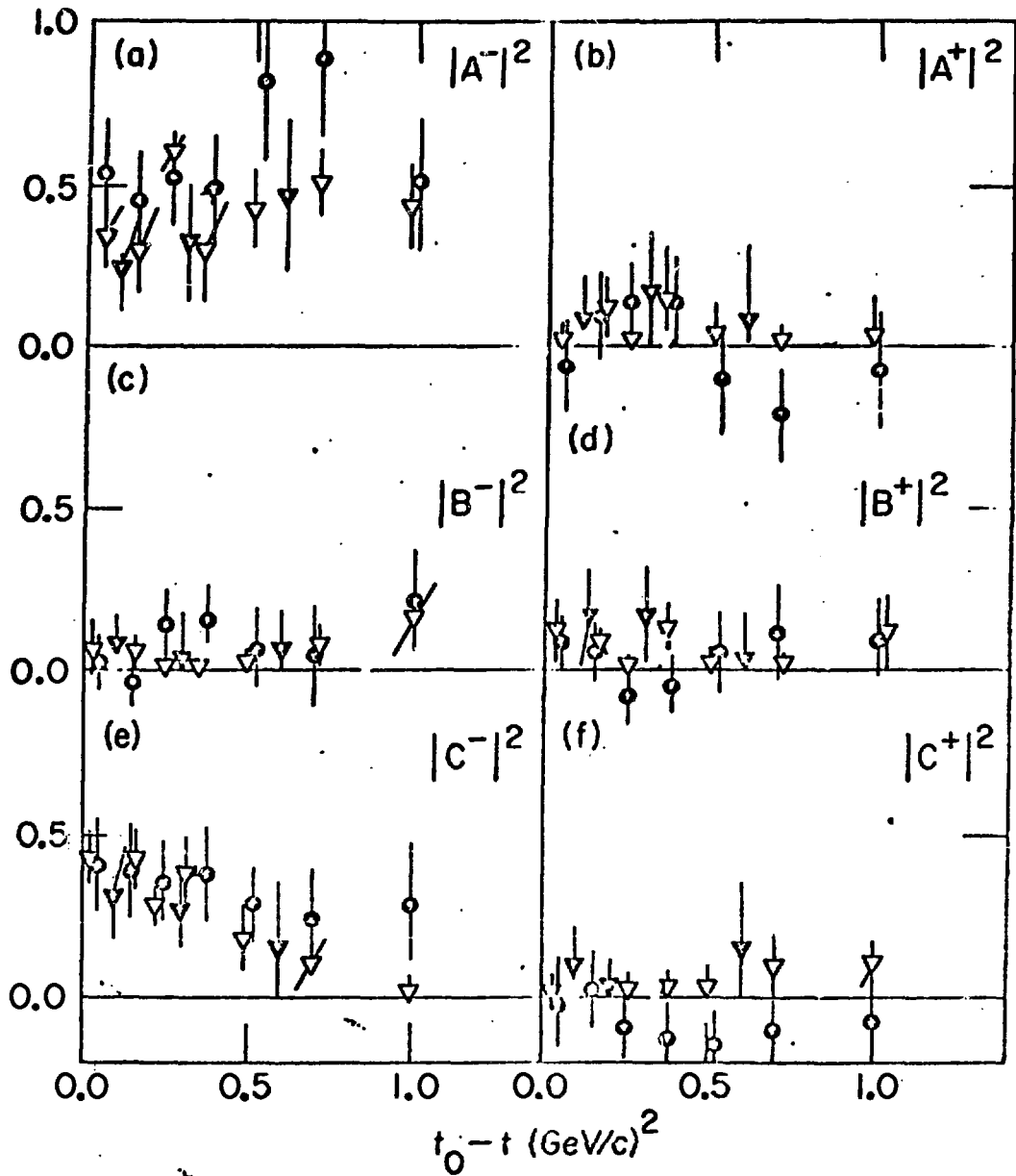


Fig. 5

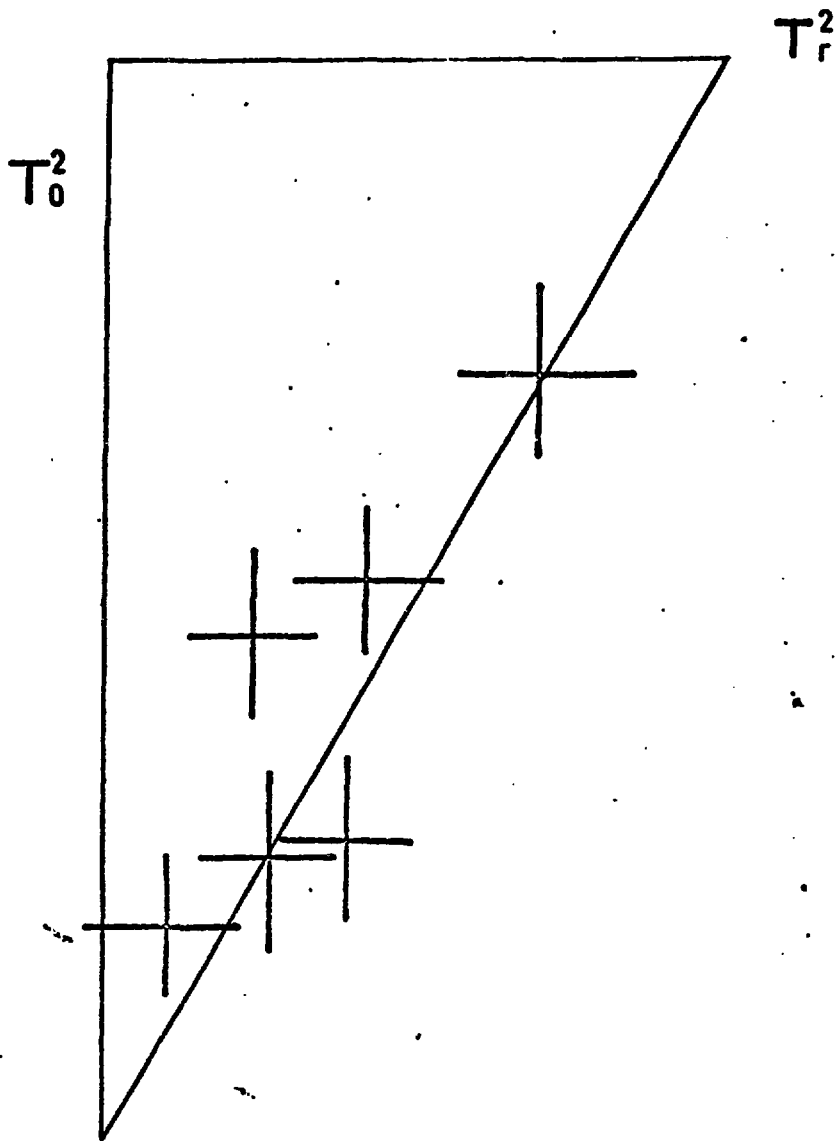
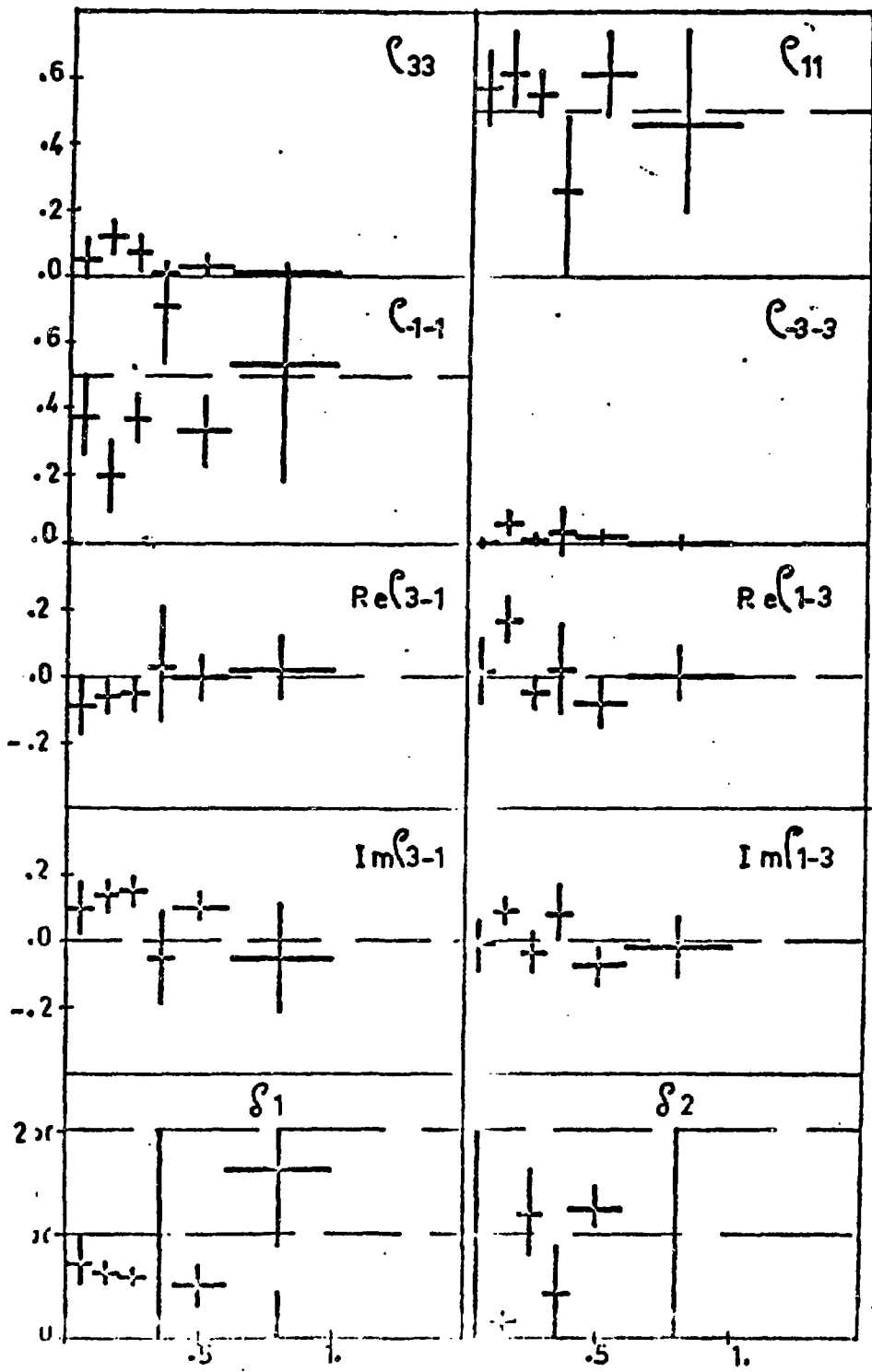


Fig. 6



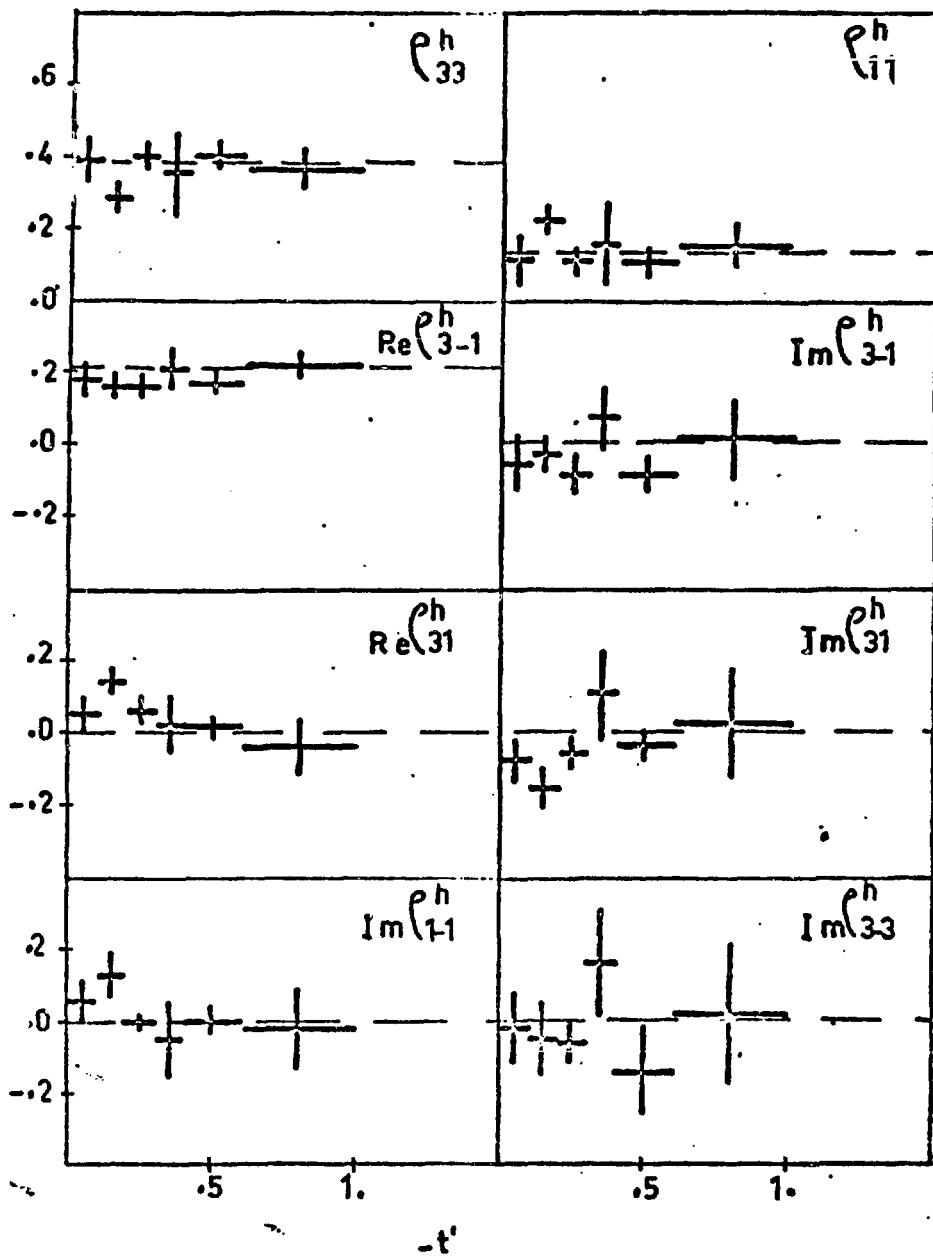


Fig. 8